Annals of Biomedical Engineering, Vol. 39, No. 12, December 2011 *(© 2011)* pp. 2945–2954
DOI: 10.1007/s10439-011-0381-7

Finger Impedance Evaluation by Means of Hand Exoskeleton

ANGELO EMANUELE FIORILLA, FRANCESCO NORI, LORENZO MASIA, and GIULIO SANDINI

Department of Robotics, Brain and Cognitive Sciences, Italian Institute of Technology, Via Morego, 30, 16163 Genoa, Italy

(Received 16 March 2011; accepted 5 August 2011; published online 24 August 2011)

Associate Editor Thurmon E. Lockhart oversaw the review of this article.

Abstract—Modulation of arm mechanical impedance is a fundamental aspect for interaction with the external environment and its regulation is essential for stability preservation during manipulation. Even though past research on human arm movements has suggested that models of human finger impedance would benefit the study of neural control mechanisms and the design of novel hand prostheses, relatively few studies have focused on finger and hand impedance. This article touches on the two main aspects of this research topic: first it introduces a mechanical refinement of a device that can be used to effectively measure finger impedance during manipulation tasks; then, it describes a pilot study aimed at identifying the inertia of the finger and the viscous and elastic properties of finger muscles. The proposed wearable exoskeleton, which has been designed to measure finger posture and impedance modulation while leaving the palm free, is capable of applying fast displacements while monitoring the interaction forces between the human finger and the robotic links. Moreover, due to the relatively small inertia of the fingers, it allows us to meet some stringent specifications, performing relatively large displacements (~45°) before the stretch reflex intervenes (~25 ms). The results of measurements on five subjects show that inertia, damping, and stiffness can be effectively identified and that the parameters obtained are comparable with values from previous studies.

Keywords—Impedance, Dexterous manipulation, Hand exoskeleton, Grasp modeling.

INTRODUCTION

Mechanical impedance is the force resistance to perturbations of state. In the field of motor control, modulation of the arm's mechanical impedance is one of the key aspects underlying neural control of interaction with the external environment. Regulating it is the fundamental factor in stability preservation during manipulation tasks.[12]

In 1985, the seminal work of Mussa-Ivaldi *et al.*[17] proposed a novel experimental paradigm using a computer-controlled mechanical interface to measure and represent the elastic force field associated with the posture of the arm. It consisted in observing the steady-state force responses to a series of separate "step" perturbations imposed in different directions. It was found that the endpoint stiffness of the human arm in the horizontal plane was primarily "spring-like" and that limb geometry had a major effect on the magnitude and directionality of endpoint stiffness. A further step towards comprehension of impedance modulation was given by Burdet *et al.*,[3] who developed an algorithm to observe impedance modulation during an unstable reaching task.

Since then, studies on measuring human impedance have focused primarily on the stiffness of the arm and the wrist[2,13,19,20] and most of the literature refers to the widely used technique of step perturbation or stochastic perturbations proposed by Bennett *et al.*[1] and Lacquaniti *et al.*[15]

A time-domain and frequency-domain identification technique for linear, multiple-input and multiple-output (MIMO) systems was also adopted to estimate the dynamic endpoint stiffness of a multijoint limb.[18]

Due to the complex anatomy of the distal part of the arm, few studies on modeling human grasps have investigated hand impedance. In these experiments, different kinds of devices have been used: pneumatically/electrically actuated platforms,[11,14,16] vibrational devices,[8] or just commercial exoskeletons.[7]

In 1997, Hajian *et al.*[11] studied the mechanical impedance of the human index finger metacarpal joint in extension and abduction. Using a small pneumatic piston they applied one-dimensional perturbation forces to the fingertip between 2 and 20 N in the extension direction and between 2 and 8 N in the abduction

Address correspondence to Angelo Emanuele Fiorilla, Department of Robotics, Brain and Cognitive Sciences, Italian Institute of Technology, Via Morego, 30, 16163 Genoa, Italy. Electronic mail: emanuele.fiorilla@iit.it

direction, then they used a linear second order model of the finger and a least-square fit to identify finger inertia, damping, and stiffness.

Still in 1997, studying calibration methods for robotic hands, Kao and Cutkosky[14] investigated the stiffness of the grasp. They proposed an algorithm to identify a stiffness matrix using a least-square fit method on experimental data recorded during pinch grasps. The device employed was made by a couple of sensorized disks driven by a torque motor. They found that non-conservative components of the stiffness matrices are negligible during human grasping.

Another apparatus for measuring the stiffness of a single finger is described in Milner and Franklin.[16] By means of the "step perturbation" method, the authors succeeded in separating conservative and non-conservative stiffness terms. The results of this study confirmed that the influence of non-conservative effects is negligible as its contribution to the total force response to static displacements is less than 15%.

In 2005, Fu and Oliver[8] studied the mechanical impedance of the index finger using a Polytec PSV-300 laser scanning vibrometer for velocity measurements and a B&K Minishaker to generate the sinusoidal force loads applied to the finger. Starting from the same linear, second order model presented by Hajian and Howe[11] demonstrated that in the range of 0.05 to 0.5 N there is no evidence of a shift in impedance behavior and that the impedance data are relatively comparable within the error of the measurements.

Recently, Friedman[7] used a setup made of a CyberGlove and a CyberGrasp, respectively, a motion capture glove and a hand exoskeleton both produced by Immersion, in order to study grasp kinematics and stiffness during object manipulation. They measured a 3D stiffness ellipsoid of the grasp during the reaching phase and stated that velocity and force transmission ellipsoids are a function of hand posture, and consequently that the stiffness of the grasp is also dependent on hand posture.

Although these experiments led to a wider comprehension of the biomechanics of hand impedance modulation, none of the devices used allowed us to measure single joint finger impedance during manipulation tasks.

This article first presents a mechatronic system (1) able to apply perturbations that are fast enough to prevent any spinal reflex occurrence during data acquisition and (2) equipped with a direct drive mechanical transmission limiting the intrinsic compliance that could affect finger impedance measurement. We present the mechanical refinement of our first version of a hand exoskeleton, which was previously presented elsewhere.[6] We highlight the enhancement in its metrological performance, and provide a method for estimating finger impedance while maintaining posture.

A pilot study then estimates the inertial, viscous, and elastic properties of the joint.

MATERIAL AND METHODS

Apparatus

The device proposed for measuring finger impedance (see Fig. 1) is a wearable robot designed to overimpose mechanical perturbations to the index finger and the thumb of a subject's hand. The exoskeleton described below is an enhancement of a previous design already presented in Fiorilla *et al.*[6]

The modifications relative to the previous design have three main goals: (1) to improve the mechanical coupling between the hand and the exoskeleton, limiting backlash and joint misalignment, (2) to tune the force measurement range and, at the same time, (3) to increase user safety while performing the experiment.

As already discussed, the device has been designed to measure passive and active finger impedance during manipulation tasks. Experiment specifications require the device to be minimally invasive and sufficiently fast because in order to estimate steady-state impedance, it is necessary for the subject not to change his/her finger impedance in response to the applied perturbation *during* data collection.

Remarkably, each human finger is a complex structure with roughly four degrees of freedom distributed on the carpometacarpal, metacarpophalangeal, and proximal/distal interphalangeal joints. In order to reduce overall device complexity it was decided to estimate impedance only in the thumb and index fingers; these two fingers play a crucial role in most types of grasping configurations (e.g., pinch grasp, lateral grasp, cylindrical, spherical, etc.). Moreover, in consideration of the complexity of each finger, it was decided to apply perturbations only at the flexion/extension metacarpophalangeal joints, therefore, leaving the interphalangeal joints and the adduction/abduction metacarpophalangeal joint unperturbed.

The final design for each finger consists of a rigid 3-link direct driven underactuated serial mechanism: a single motor for each of the 3-link chains actuates the proximal link while the middle and distal links work as force transmission elements (see Fig. 1a). The motors are mounted on a base at the back of the palm and are able to slide on a rail and rotate around the vertical axis to compensate for any joint misalignment. Once a proper alignment is achieved, the linear slider and the rotational free joint can be blocked in a comfortable configuration for the subject (see Fig. 1d). A

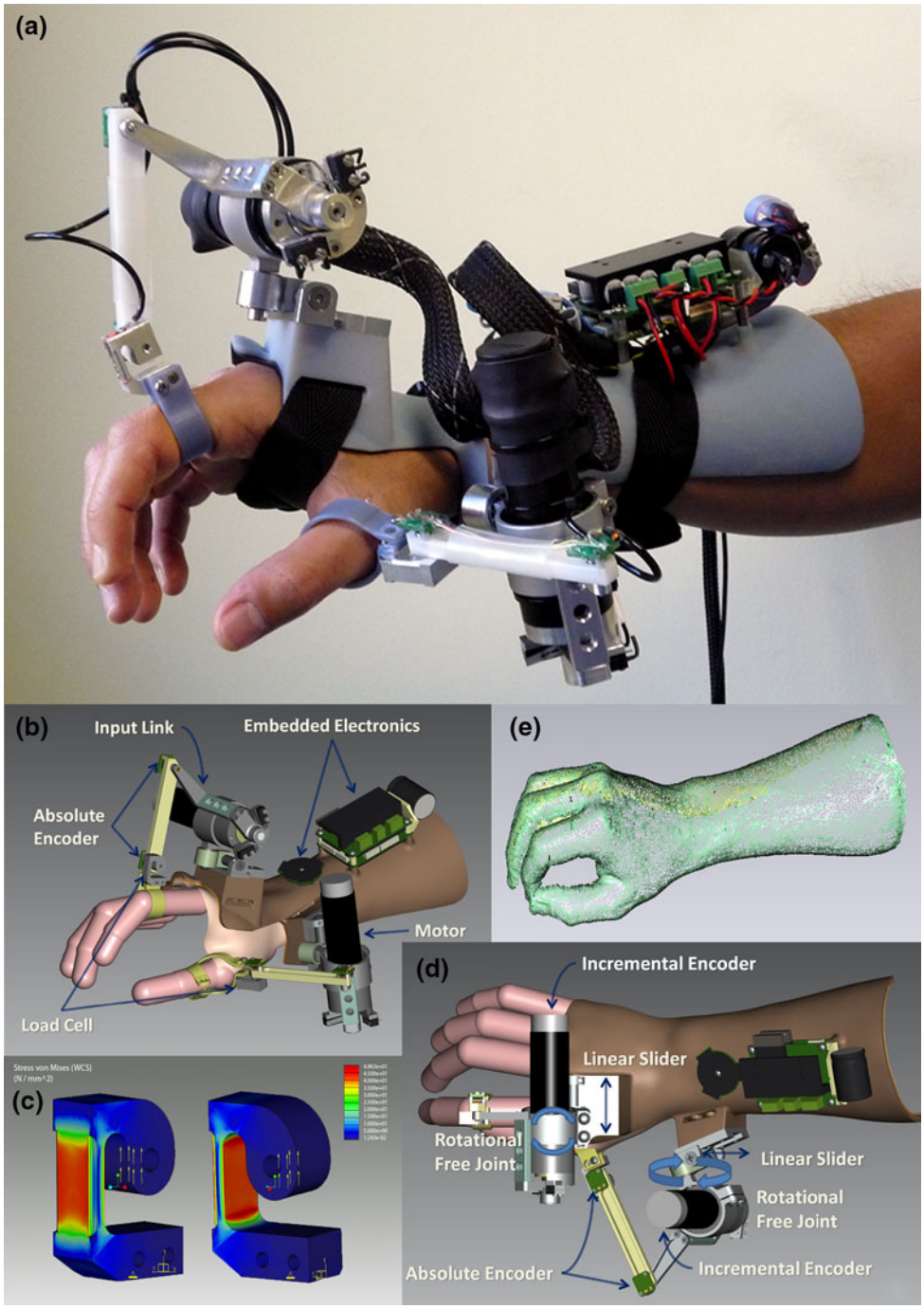

FIGURE 1. The final aspect of the assembled exoskeleton (a) as well as the most important phases of its design (b–d). (b, d) A CAD perspective view and a top view of the device, pointing to the main parts of the device. (c) The result plot of the finite element modeling (FEM) analysis conducted on the custom load cell; it shows the spot on the load cell where the maximum deformation occurs and obviously the best location to glue the semiconductor strain-gauges on. (e) A point cloud representation of a 3D scanned forearm; a medium size forearm has been digitalized to give the exoskeleton an anatomical support.

mathematical representation of the device kinematics is presented in Appendix A.

The assembled device is made to be worn by the subject on the dorsal part of the hand. In order to solve coupling problems between the device and the dorsal side of the forearm, which affected the previous model of the exoskeleton, the *support* was designed by means of a 3D scan of a real forearm (see Fig. 1e) and then realized using a multiple layer 3D printer (a Connex350® from Object Geometries Ltd.). The internal layer (the one in contact with the forearm) is made of a soft rubber-like flexible material (TangoBlack) while

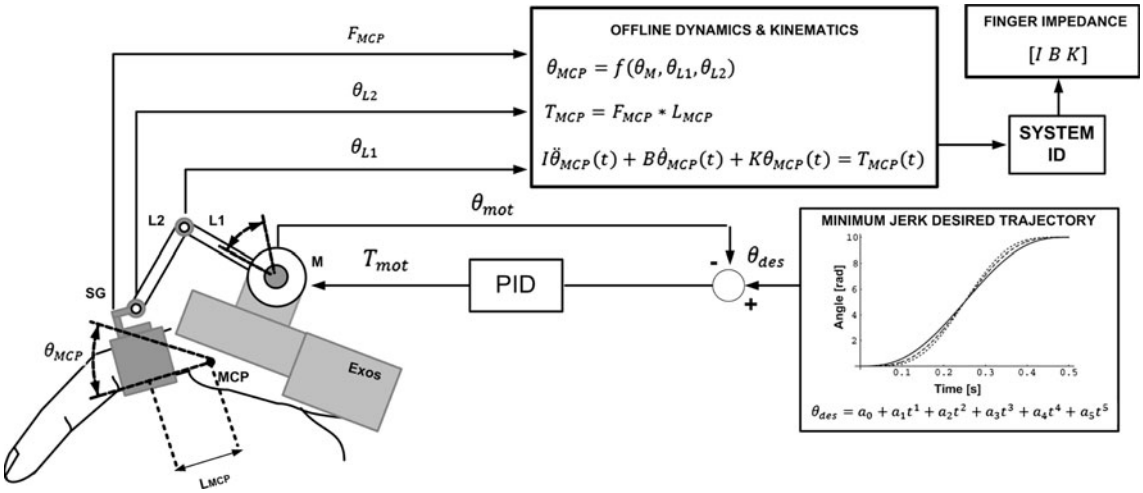

FIGURE 2. The exoskeleton control block diagram. In the lowest section of the schema, the high-level part of the control system generates minimum jerk trajectories from the actual position to the desired position and the low-level part of the controller makes the motor "follow" the trajectory. At the same time, another part of the control board (upper section of the schema) acquires position and force data from the sensors in order to identify the parameters of the dynamic model (i.e., inertia, damping, and stiffness).

the external layer (where the exoskeleton is attached) is made of a hard opaque material (VeroGray).

Regarding the *actuators*, the same hardware that had been chosen for the previous exoskeleton has also been mounted on the new device. Simulations involving the main static and dynamic components of motion and practical experiments demonstrated that these motors are adequate for our goals.[6] The critical specification for the chosen actuators was the ability to displace a finger (of approximate inertia 5.0×10^{-6} kg m^2 and mass 0.025 kg) by 45° in 25 ms to avoid influences from spinal reflexes.

Each actuator consists of a brushed DC motor,[1] assembled with a 14:1 ceramic planetary gearbox and a magnetic rotary encoder.[2] The motor has a nominal speed of 8360 rpm and can exert a continuous torque equal to 26.7 mNm, and a stall torque up to 257 mNm.

The 3-link structure moving each finger plus the "finger link" make a four-bar linkage in a crank-slider configuration (see Fig. 2). This configuration has just one degree of freedom and the angle of the finger's MCP joint (follower link) is unambiguously related to the angle of the link actuated by the motor (input link). From the previous device, however, the new exoskeleton design inherited redundant absolute position sensors that are mounted at different joints of the parallelogram and are based on the integrated circuit AS5045 from Austriamicrosystems[3] (see Figs. 1b, 1d).

In order to measure the interaction forces between the finger and the device, the most distal link of the exoskeleton is equipped with a customized load cell, optimized in terms of ranges and signal-to-noise ratio to be adequate for the specific application. The load cell is made of Aluminium 7075 (ergal) and is the size of the elements chosen so that it has a linearity range between ±20 N (±0.6 Nm torque on the finger MCP joint) and a weakening over ±100 N (±3 Nm torque applied on the MCP joint). A finite element method (FEM) stress analysis was conducted on the parts that were then sensorized using two semiconductor strain-gauges[4] in a half-bridge electrical configuration (see Fig. 1c).

As a final remark, it is important to highlight the reason why such a sensor-redundant choice was made: notice that in our current analysis we are interested in the force component directly acting on the finger joint and therefore generating the torque and laying in the plane of the finger's passive movement (i.e., the component directly projecting on the MCP flexion/extension joint). The force sensor, however, is also sensitive to a parallel component, which is not relevant for the analysis. In order to minimize the effect of the parallel component, an optimization of the four-bar linkage geometry was performed. This optimization maximized the normal component in a range of movements

[1]The motors used in this device are Maxon RE 25 (∅25 mm, graphite brushes, 20 W brushed DC motor), available from http://shop.maxonmotor.com/ishop/article/article/118752.xml

[2]The encoder mounted on the motor's shaft is a 3 channel rotary encoder. Its resolution is equal to 1000 CPT (Count per Turn).

[3]Austriamicrosystems AS5045 12-bit programmable magnetic rotary encoder.

[4]Micron Instruments semiconductor backed gauges.

that corresponds to 50 degrees of the finger flexion/extension MCP joint.

Finally, in order to increase user safety, electronic switches were installed on the mechanical stops. They are essential for preventing injuries to the subject's fingers and motor burn out.

Experiment

The experiments aim to collect information about the dynamic characteristics of fingers. Data were recorded during passive finger motion and post processed to identify the inertia, damping, and stiffness coefficients that describe the dynamic behavior of the index fingers and the thumb. The idea is to evaluate the contribution of the three terms mentioned above in the reconstruction of the whole finger impedance.

Recordings were carried out on five healthy right-handed, male subjects, with an average age of 29.3 ± 0.2 years. The subjects were comfortably seated with their right hands laying semipronated on a foam layer. The experiments consisted in five sessions, of 20 trials each. Five different motor velocities, equally spaced between 0.75 and 45 rad/s, were set and an extension movement was applied 20 times to the subject's index finger and thumb. A 10-s time interval between one trial and the next was introduced to allow the subject to relax the forearm muscles, as well as to avoid fatigue and adaptation. Each subject was instructed "not to intervene voluntarily".

A plot of measured displacements and torques is depicted in Fig. 3. It shows mean ± standard deviation values of angular displacement (blue shadings) and torque (red shadings) for the five velocities applied to the finger.

Even though the torque data that were used to compute finger impedance include both the contribution of soft tissues, and muscles and tendons of the

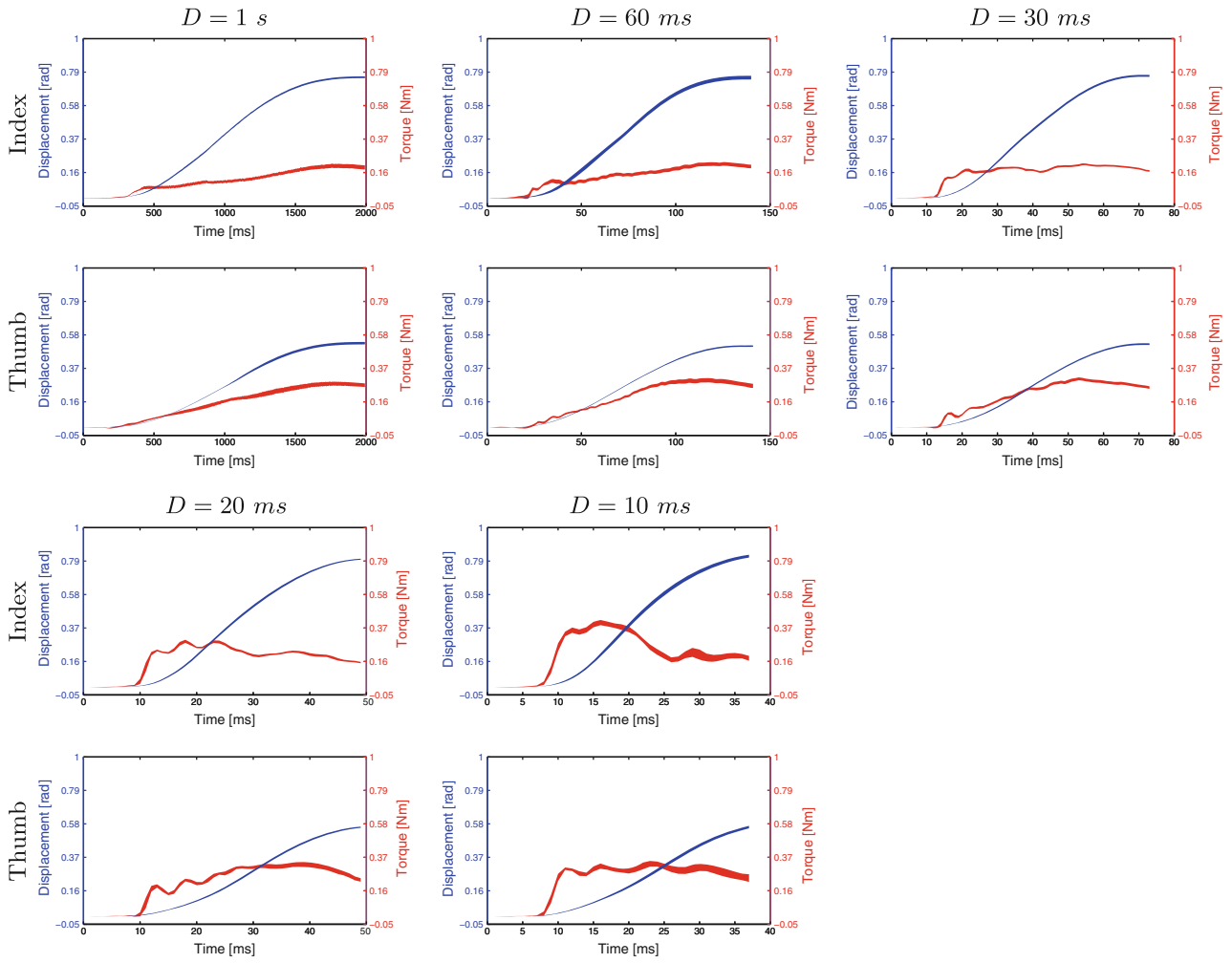

FIGURE 3. The position and torque data acquired from one subject for the five different values of the minimum jerk trajectory time length ($D = t_f - t_0$). The mean ± standard deviation values of position and torque are depicted as colored shading. In each subplot, the left blue axis refers to position (blue shading) and the right red axis refers to torque (red shading).

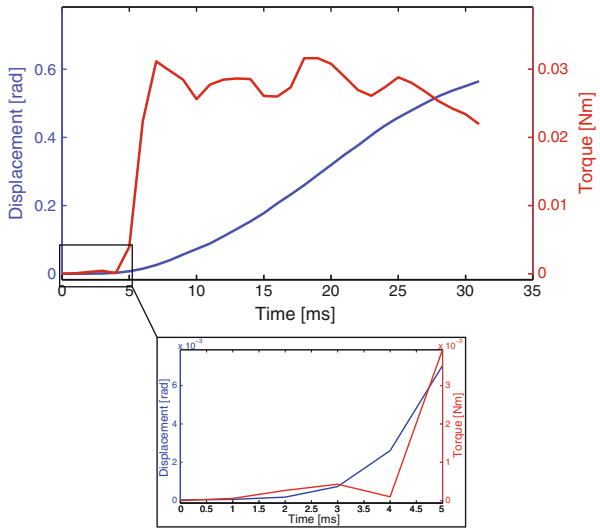

FIGURE 4. Displacement and torque plot for a single trial: the magnified part of the upper plot highlights the contribution given to total impedance by the elasticity of soft tissues.

finger as they were recorded during the whole motion, we can state confidently that the soft tissues term did not significantly affect the measurement. As a matter of fact, the smallest contribution given to the total impedance by soft tissues can be spotted during the first few milliseconds of motion. As shown in Fig. 4, once the thin skin of the finger is completely compressed, its contribution is minimal. Moreover, in 2005, Dong *et al.*[5] studied the biodynamic response at the palm of the human hand subjected to a random vibration and claimed that "at low frequencies (<40 *Hz*), the palm cannot effectively isolate vibration, so the vibration can be effectively transmitted to the entire hand-arm system". As soft tissues of the finger are thinner than those of the palm we can likely extend this result to the finger too.

Identification Algorithm

A standard linear time-invariant equation of motion can be used to identify the mechanical impedance of a one-DoF rotational system (e.g., the flexion/extension MCP joint of the index finger) and consequently separate the contribution given by inertia, damping, and stiffness:

$$I\ddot{\theta}(t) + B\dot{\theta}(t) + K\theta(t) = \tau(t) \qquad (1)$$

where $\theta, \dot{\theta}, \ddot{\theta}$ are angular position, velocity, and acceleration, τ is external torque, I is constant mass parameter, B is constant damping, and K is stiffness constant.

Generally, in order to estimate the instantaneous inertia, damping and stiffness values, the system is perturbed by an external torque measured by the load cell $\tau(t)$ and the motion response over time $(\theta(t), \dot{\theta}(t), \ddot{\theta}(t))$ is measured. Then, repeating the protocol and using a least-squares fit, an overall estimation of the three parameters (I, B, K) can be obtained.

For this specific experiment, we chose to impose a position perturbation and to measure the restoring torque.

Before fitting the experimental data to the dynamic model (1), a preliminary system identification process was performed to clean trajectories as well as velocity and acceleration data from mechanical noise. This "filtering" process takes advantage of the fact that position commands are numerically generated by the control board as minimum jerk profiles, moving from the current position to the desired position.

The method proposed in this article considers this information about the motion characteristics to identify the parameters that optimally fit the minimum jerk trajectory (a least mean square (LMS) identification algorithm is used), which has been measured on the finger MCP joint. Once the minimum jerk coefficients are estimated, velocity and acceleration are computed by algebraic derivation from the motion profile obtained: they are smoother than the noisy velocity and acceleration profiles that could be obtained numerically deriving from the position data (see Fig. 5).

RESULTS

In order to study the contribution of inertia (I), damping (B), and stiffness (K) to interaction torques measured by the device, the standard linear time-invariant equation of motion (1) was used to estimate the three terms (a LMS algorithm was applied). First, we estimated torque by using three different "versions" of the equation (1) that, respectively, take into consideration $\{I, B, K\}$, $\{B, K\}$, and only $\{K\}$. The aim of this analysis was to identify the contribution of each term and the quality of the system identification. A plot of measured and estimated torques in the three above-mentioned cases is shown in Fig. 6. Moreover, the mean square error (MSE) of torque estimation is reported in Table 1.

Figure 6 shows that as expected, the contribution given by the inertial and damping terms is more considerable at the highest speeds while they do not improve the quality of estimation much at the lowest speeds. The reason for this outcome is that at the lowest speeds, velocity and acceleration terms are negligible as they cannot be perfectly distinguished from measurement noise.

For this reason, the quality of fitting varies from one session to another according to the speed of perturbation. In this specific case, in order to provide a

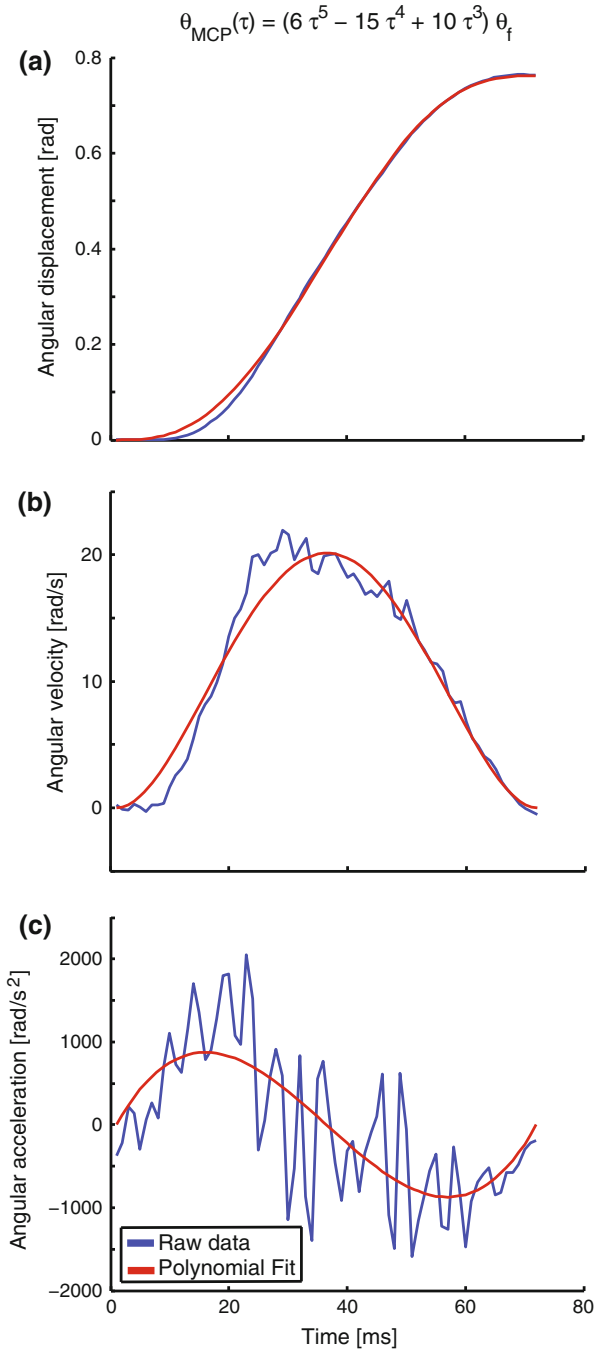

FIGURE 5. A plot of the finger's angular position measured during a single trial (a) as well as the velocity (b) and acceleration (c) data obtained numerically from the position data (blue line). A plot of the "filtered" position data obtained through a Minimum Jerk polynomial fit and of the velocity and acceleration data obtained algebraically from the polynomial expression (red line) was superimposed on each graph. As shown, the "filtered" profiles constitute a good approximation of the noisy, numerically obtained, profiles of velocity and acceleration.

comprehensive representation of the dynamics of the system, this article presents only the parameter values that were obtained by using the $\{I, B, K\}$ model; hence, position, speed, acceleration, and force data measured by the device were used to identify inertia, damping, and stiffness of the fingers.

The obtained outcomes of the index finger and thumb are presented in Table 2. As stated before, some parameter incongruences in the Table (i.e., inertia values that are several orders of magnitude higher at the lowest speed than at higher speeds and, just in one case, negative) have to be ascribed to the low sensitivity and quantization of force sensors and encoders that do not allow one to perfectly distinguish the lowest velocities and accelerations from measurement noise.

DISCUSSION

Impedance modulation is a fundamental mechanism for describing how humans physically interact with the external environment. The inherent spring-like properties of muscles are beneficial for many reasons, for example, they are able to prevent instability and to filter external disturbances by increasing or decreasing the muscle tone. Even though it has been stated that having models of human finger impedance could really shed some light on the complex strategy of interaction and control of the distal part of the human arm, relatively few studies have investigated finger and hand impedance in humans.

Previous studies[3,9,17] have been mostly focused on measuring the impedance of the arm while maintaining posture or during reaching tasks. However, the results of these studies do not include any impedance measurements of the distal arm (hand and wrist). As a matter of fact, the role of the hand and wrist is fundamental in daily life activities and there is strong evidence that impedance modulation of the distal and proximal limb are decoupled. Sharon[21] hypothesized a biologically plausible sub-division of the human arm in two main assemblies characterized by different inherent dynamic behaviors: a macro-manipulation system mainly associated to the proximal limb shoulder and elbow and a micro-manipulation system made by the anatomical distal part of the wrist and hand; the macro-system is responsible for interaction with heavy loads at low frequencies, the micro-system is more devoted to fine interaction and manipulation, which require higher frequencies and smaller forces. This kind of macro/micro-architecture would be beneficial because the overall dynamic behavior is inherently more stable in regulating force at the interface during manipulation tasks. This is because the whole system is more prone to matching its impedance with that of the external environment and therefore rejecting the disturbances. In terms of manipulation dexterity, the hand and wrist allow modulation of impedance at the

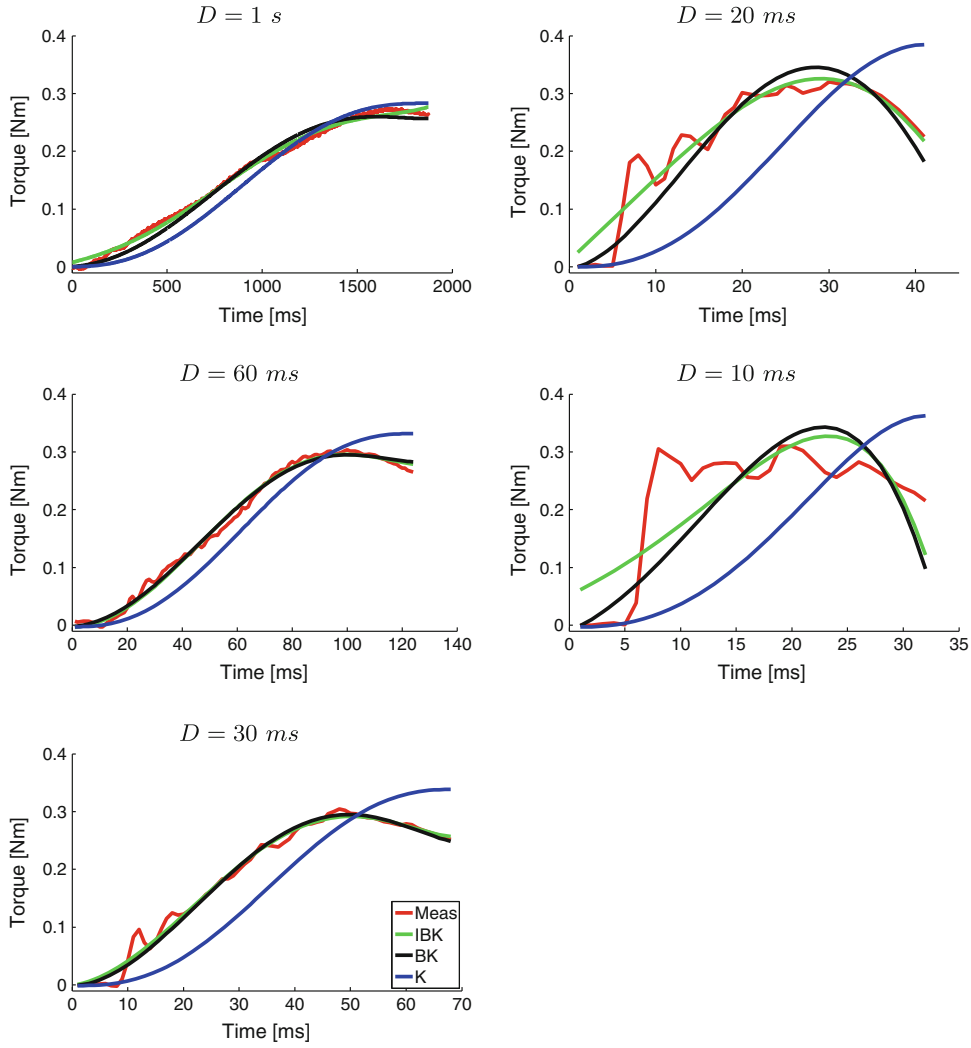

FIGURE 6. Measured and estimated torque plot. In order to estimate the contribution of inertia, damping, and stiffness in reconstruction of measured torques, different "versions" of Eq. (1) were used. The figure shows the measured and the estimated torques obtained from the different models ({*I*, *B*, *K*}, {*B*, *K*}, and {*K*}) at the different values of the minimum jerk trajectory time length ($D = t_f - t_0$). It can be seen that while the model of stiffness alone can estimate quite precisely the torque at the minimum velocity, this term alone is not enough to approximate the measured data for higher velocities.

TABLE 1. The mean square error (MSE) of torque estimation obtained by three different dynamic models for different values of the minimum jerk trajectory time length ($D = t_f - t_0$).

D (ms)	*IBK* $(Nm)^2$	*BK* $(Nm)^2$	*K* $(Nm)^2$
Index finger			
1000	0.6251	1.1540	2.6735
60	3.2217	4.2891	5.9337
30	1.4617	1.8080	3.4332
20	5.6067	5.7317	13.2619
10	0.4616	0.6443	2.0868
Thumb			
1000	1.5868	1.9714	5.4817
60	2.7408	3.2217	5.2701
30	0.8559	0.0932	2.1349
20	1.8657	2.1734	4.0680
10	1.7118	1.9426	4.6834

end-effector almost independently from the shoulder and elbow joint, providing redundant possibilities to approach the required task.

Multiple questions arise: is the nature of the task responsible for impedance modulation strategy? Are distal (micro) and proximal (macro) arms' impedances decoupled?

This article presents a wearable device developed to perform measurements of finger impedance in static conditions as well as during complex manipulation tasks. This manuscript is focused on showing the details of the main design and construction phases and on describing an experiment that was performed to investigate the muscle tone of human fingers. The aim of this experiment was to separate the different

TABLE 2. The dynamic parameters (inertia, damping, and stiffness) as they were identified using the dynamic model in Eq. (1).

D (ms)	Inertia (kg m^2)	Damping (kg m^2/s)	Stiffness (Nm/rad)
Index finger			
1000	$(1100 \pm 751) \times 10^{-6}$	$(-3100 \pm 6100) \times 10^{-6}$	0.49 ± 0.24
60	$(5.31 \pm 7.49) \times 10^{-6}$	$(64.6 \pm 370) \times 10^{-6}$	0.59 ± 0.31
30	$(2.40 \pm 1.47) \times 10^{-6}$	$(454 \pm 115) \times 10^{-6}$	0.51 ± 0.26
20	$(2.59 \pm 0.769) \times 10^{-6}$	$(552 \pm 119) \times 10^{-6}$	0.47 ± 0.24
10	$(2.98 \pm 0.98) \times 10^{-6}$	$(613 \pm 208) \times 10^{-6}$	0.48 ± 0.19
Thumb			
1000	$(764 \pm 1200) \times 10^{-6}$	$(-631 \pm 6000) \times 10^{-6}$	0.44 ± 0.17
60	$(-1.81 \pm 5.80) \times 10^{-6}$	$(391 \pm 526) \times 10^{-6}$	0.49 ± 0.19
30	$(1.88 \pm 1.07) \times 10^{-6}$	$(715 \pm 209) \times 10^{-6}$	0.45 ± 0.15
20	$(6.36 \pm 2.68) \times 10^{-6}$	$(454 \pm 351) \times 10^{-6}$	0.60 ± 0.31
10	$(3.56 \pm 2.58) \times 10^{-6}$	$(610 \pm 432) \times 10^{-6}$	0.49 ± 0.20

Each row contains the parameter values that were obtained for a given value of the minimum jerk trajectory time length ($D = t_f - t_0$).

components of measured finger torque by describing its dynamic behavior. This article opens opportunities to investigate the human arm as a double system; in fact the proposed device can be easily plugged into a planar manipulator and the different contributions in impedance of distal and proximal arms can be discriminated while performing a reaching task or even during the reaching phase associated to a grasping task.

The preliminary results obtained, which can be considered consistent by subject and displacement velocity, show that inertia, damping, and stiffness can be effectively identified using the proposed device and method and that, apart from some issues emerging at the lowest speed, the parameter values obtained are comparable with values from classical literature[4,22] and previous research results.[7,10,11,16]

Advantages from this kind of investigation can be beneficial for many research areas: for example, next generation robotic hands and prostheses could be designed considering human measurements to optimize ergonomics due to their ability to change passive compliance and, hopefully, to make them capable of mimicking human behavior.

APPENDIX A: EXOSKELETON FINGER KINEMATICS—DENAVIT–HARTENBERG REPRESENTATION

The kinematics of the mechanical chain that actuates each finger can be represented using the Denavit–Hartenberg convention in Table 3.

L_0, L_1, L_2, and L_3 are the distances between the finger MCP joint and the motor shaft and the length of the three joints of the exoskeleton, while θ_1, θ_2, θ_3, and θ_4 are the angles of the motor cantilever and of the three joints of each finger of the exoskeleton (see Fig. 7).

TABLE 3. Denavit–Hartenberg parameters for the exoskeleton finger links.

Link	a_i	α_i	d_i	θ_i
1	0	$\pi/2$	L_0	θ_1
2	L_1	0	0	θ_2
3	L_2	0	0	θ_3
4	L_3	0	0	θ_4

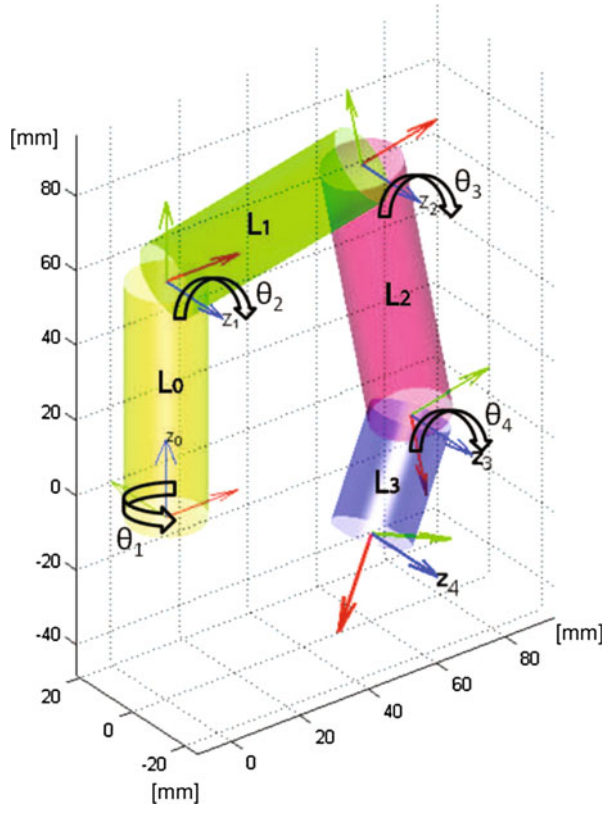

FIGURE 7. A diagram of the exoskeleton finger kinematics. The axes are arranged according to the Denavit–Hartenberg convention.

ACKNOWLEDGMENTS

This work was partially funded by the European Commission's Sixth Framework Programme as part of the VIACTORS project under Grant no. 231554. We want to acknowledge the RobotCub consortium for designing and maintaining the development of the electronic devices included in this project.

REFERENCES

[1]Bennett, D. J. Torques generated at the human elbow joint in response to constant position errors imposed during voluntary movements. *Exp. Brain Res.* 95(3):488–498, 1993.

[2]Bennett, D. J., J. M. Hollerbach, Y. Xu, and I. W. Hunter. Time-varying stiffness of human elbow joint during cyclic voluntary movement. *Exp. Brain Res.* 88(2):433–442, 1992.

[3]Burdet, E., R. Osu, D. Franklin, and M. Kawato. The central nervous system stabilizes unstable dynamics by learning optimal impedance. *Nature* 414(6862):446–449, 2001.

[4]Chao, E. Y. S., K.-N. An, W. P. Cooney, and R. L. Linscheid. Biomechanics of the Hand—A Basic Research Study. Singapore: World Scientific Publishing Company, 1989.

[5]Dong, R. G., T. W. McDowell, and D. E. Welcome. Biodynamic response at the palm of the human hand subjected to a random vibration. *Ind. Health* 43(1):241–255, 2005.

[6]Fiorilla, A. E., N. G. Tsagarakis, F. Nori, and G. Sandini. Design of a 2-finger hand exoskeleton for finger stiffness measurements. *Appl. Bionics Biomech.* 6:217–228, 2009.

[7]Friedman, J., and T. Flash. Task-dependent selection of grasp kinematics and stiffness in human object manipulation. *Cortex* 43(3):444–460, 2007.

[8]Fu, C., and M. Oliver. Direct measurement of index finger mechanical impedance at low force. First Joint Eurohaptics Conference, 2005 and Symposium on Haptic Interfaces for Virtual Environment and Teleoperator Systems, 2005. World Haptics 2005, pp. 657–659, 2005. doi:10.1109/WHC.2005.40.

[9]Gomi, H., and M. Kawato. Human arm stiffness and equilibrium-point trajectory during multi-joint movement. *Biol. Cybern.* 76(3):163–171, 1997.

[10]Grinyagin, I. V., E. V. Biryukova, and M. A. Maier. Kinematic and dynamic synergies of human precision-grip movements. *J. Neurophysiol.* 94(4):2284–2294, 2005. doi:10.1152/jn.01310.2004.

[11]Hajian, A. Z., and R. D. Howe. Identification of the mechanical impedance at the human finger tip. *J. Biomech. Eng.* 119(1):109–114, 1997.

[12]Hogan, N. The mechanics of multi-joint posture and movement control. *Biol. Cybern.* 52(5):315–331, 1985.

[13]Jones, L. A., and I. W. Hunter. Influence of the mechanical properties of a manipulandum on human operator dynamics. 1. Elastic stiffness. *Biol. Cybern.* 62(4):299–307, 1990.

[14]Kao, I., M. Cutkosky, and R. Johansson. Robotic stiffness control and calibration as applied to human grasping tasks. *IEEE Trans. Robotics Autom.* 13(4):557–566, 1997. doi:10.1109/70.611319.

[15]Lacquaniti, F., M. Carrozzo, and N. A. Borghese. Time-varying mechanical behavior of multijointed arm in man. *J. Neurophysiol.* 69(5):1443–1464, 1993.

[16]Milner, T., and D. Franklin. Characterization of multijoint finger stiffness: dependence on finger posture and force direction. *IEEE Trans. Biomed. Eng.* 45(11):1363–1375, 1998. doi:10.1109/10.725333.

[17]Mussa-Ivaldi, F. A., N. Hogan, and E. Bizzi. Neural, mechanical, and geometric factors subserving arm posture in humans. *J. Neurosci.* 5(10):2732–2743, 1985.

[18]Perreault, E. J., R. F. Kirsch, and A. M. Acosta. Multiple-input, multiple-output system identification for characterization of limb stiffness dynamics. *Biol. Cybern.* 80(5):327–337, 1999.

[19]Pisano, F., G. Miscio, R. Colombo, and P. Pinelli. Quantitative evaluation of normal muscle tone. *J. Neurol. Sci.* 135(2):168–172, 1996.

[20]Serres, S. J. D., and T. E. Milner. Wrist muscle activation patterns and stiffness associated with stable and unstable mechanical loads. *Exp. Brain Res.* 86(2):451–458, 1991.

[21]Sharon, A. The Macro/Micro Manipulator: An Improved Architecture for Robot Control. Ph.D. thesis, Department of Mechanical Engineering, Massachusetts Institute of Technology, 1989.

[22]Tubiana, R. The Hand. Philadelphia: W.B. Saunders Company, 1981.